Int J Appl Earth Obs Geoinformation 63 (2017) 167–177

Contents lists available at ScienceDirect

Int J Appl Earth Obs Geoinformation

journal homepage: www.elsevier.com/locate/jag

Enhanced change detection index for disaster response, recovery assessment and monitoring of buildings and critical facilities—A case study for Muzzafarabad, Pakistan

Dilkushi A. de Alwis Pitts, Emily So

Department of Architecture, University of Cambridge, United Kingdom

Enhanced Change Detection Index for Disaster Response, Recovery Assessment and Monitoring of Buildings and Critical Facilities-A Case Study for Muzzafarabad, Pakistan

Authors

Dilkushi A. de Alwis Pitts[a],Emily So[a]

[a]Department of Architecture, University of Cambridge, United Kingdom

email: kad49@cam.ac.uk

Abstract The availability of Very High Resolution (VHR) optical sensors and a growing image archive that is frequently updated, allows the use of change detection in post-disaster recovery and monitoring for robust and rapid results. The proposed semi-automated GIS object-based method uses readily available pre-disaster GIS data and adds existing knowledge into the processing to enhance change detection. It also allows targeting specific types of changes pertaining to similar man-made objects such as buildings and critical facilities. The change detection method is based on pre/post normalized index, gradient of intensity, texture and edge similarity filters within the object and a set of training data. More emphasis is put on the building edges to capture the structural damage in quantifying change after disaster. Once the change is quantified, based on training data, the method can be used automatically to detect change in order to observe recovery over time in potentially large areas. Analysis over time can also contribute to obtaining a full picture of the recovery and

development after disaster, thereby giving managers a better understanding of productive management and recovery practices. The recovery and monitoring can be analyzed using the index in zones extending from to epicentre of disaster or administrative boundaries over time.

Keywords: Change Detection, Remote Sensing, Disaster Response and Recovery, Buildings, Critical Infrastructure

1. Introduction

A quicker search and rescue response following a disaster leads to a higher survival rate. That is particularly true in developing countries, because of fragile housing construction materials and technologies. Most damage assessments focus on the destruction of man-made objects, particularly buildings, to assess the survival rate. Rapid and robust damage assessment on a per-building level is essential for estimating the threat to human life (Bird and Bommer, 2004; Edrissi et al., 2013) and initiating effective emergency response and recovery actions, especially in highly populated urban areas (Vu and Ban 2010). Critical infrastructure such as hospitals and police and fire stations plays a vital role in rescue efforts, thereby increasing the survival rate.

Rescue efforts are even less effective when high priority areas pertaining to disproportionately many casualties are not clearly identified. An accurate assessment (include remote sensing) of damaged and intact roofs at building level can provide valuable information for preliminary planning of high-priority areas (focus area mapping) that is essential for rapid recovery measures (Vetrivel et al., 2016). As for other critical infrastructure, it is important to have a preliminary indication of which facilities are operational. Provided that the analyst knows where such critical facilities are, temporal analysis and change detection can be valuable tools to see the condition of the facilities soon after disaster. With a map of building and critical facilities in hand, the analyst can proceed quickly with the identification and information on damage from suitable very high-resolution (VHR) satellite imagery (Walter, 2004) by comparing data from a chosen reference before the event (pre-event) to imagery acquired shortly after the event (post-event). The availability of pre- and post-event data opens the possibility for gathering impact assessment data using change detection in complex environments such as urban areas (de Alwis Pitts and So, 2017). Change detection from high spatial-resolution images such as IKONOS and QuickBird is even more challenging, especially in complex environments characterised by small objects such as houses, individual trees and roads, and due to shadows (Pagotetal, 2008).

Nadir views generally are not accurate enough to assess building damage and collapse; however assessment results have been highly valuable (Kerle, 2010) in data-poor countries. The main problem is that conventional nadir view remote sensing does not permit assessment of damage along the façades (Gerke and Kerle, 2011a).

In general, change detection techniques can be grouped into two types: pixel-based and object-based (Blaschke, 2010; Li et al., 2011). Pixel-based change detection analysis refers to using a change detection algorithm to compare the multi-temporal images pixel-by-pixel, whereas object-based change detection analysis refers to using a change detection algorithm to compare multi-temporal images object-by-object. However, the definition of pixel-based and object-based change detection is not absolute. The most basic feature of object-based approaches is to segment the image and regard the objects as the basic unit of operation, whereas the pixel-based approach regards a single pixel as the basic unit (Daiet al., 1998).

Object-based methods have the potential to provide more accurate results than traditional pixel-based methods (Al-Khudhairy et al., 2005), but the initial step of detecting the object feature is not straightforward because the high information content of VHR images requires an accurate definition of the object. Most object-based algorithms concentrate on detecting objects such as rectangular buildings (Lin et al. 1998) or parallel lines to detect manmade objects. Cheng and Han (2016) have published a survey of more generic object detection methods for the detection of different types of objects in satellite and aerial images, such as buildings. In the literature, building detection has been achieved in single or multiple operations using methods such as morphological hit-or-miss transform (HMT)(Lefèvre et al., 2007; Stankov and He, 2013, 2014), improved snake model (Peng et al., 2005a), Discrimination by Ratio of Variance (DRV) (Lhomme et al., 2009), knowledge-based object detection methods (Akçay and Aksoy, 2010; Haala and Brenner, 1999; Hofmann et al., 2002; Huertas and Nevatia, 1988; McGlone and Shufelt, 1994; Peng and Liu, 2005; Shufelt, 1996; Stilla et al., 1997; Weidner and Förstner, 1995), context knowledge such as shadow evidence (Irvin and McKeown, 1989; Lin and Nevatia, 1998; Liow and Pavlidis, 1990; Ok, 2013; Ok et al., 2013), texture pattern features (Senaras et al., 2013), conditional random field (CRF) (Lafferty et al., 2001, Kumar and Hebert, 2003),etc. Building detection in highly complex VHR images of dense urban areas often suffers from challenges due to large variations in the visual appearance of the building caused by viewpoint variation, occlusion, background clutter, illumination, shadow, etc. (Cheng and Han, 2016). Thus the object detection step is the most complex and causes most of the error (Michaelsen et al., 2006).

Many current change-detection mechanisms do not make effective use of available pre-disaster data and existing knowledge (Guo et al., 2015). Hence using pre-disaster GIS objects such buildings as indicators allows targeting the search for specific changes to these areas within the objects of interest. The GIS object-based method discussed here is a modified version of the published work of de Alwis Pitts and So (2017) for roads and open spaces. The proposed indicator-specific method uses readily available pre-disaster GIS data and existing knowledge to enhance the detection of change while offering the possibility to target specific types of changes pertaining to similar man-made objects.

In this research a pre/post normalized index for buildings is developed, based on gradient, texture, and edge similarity filters within the buildings and an existing set of training data. The method used for buildings, although similar to the method used in de Alwis Pitts and So 2017, differs significantly in terms of the dominant attribute of change. Since edges play a large role in detecting buildings and their structural damage (Sirmacek and Unsalan, 2009). To detect buildings and damage thereto, more emphasis has been put on detecting the changes of the edges surrounding the buildings.

The proposed semi-automated method is evaluated using QuickBird datasets for abrupt changes soon after a disaster. The method could also be automated to monitor progressive changes months after a disaster. The work shown in this publication also emphasises the importance of having a good pre-disaster GIS for developing countries that are prone to disaster.

2. Method

2.1. Case Study Site

2.1.1. Muzzaffarabad, Pakistan

The Kashmir earthquakewasa destructive 7.6 Mw earthquake that struck the northwest region of Pakistan, near the city of Muzaffarabad, on 8 October 2005 at 08:52 local time (Earthquake.usgs.gov 2005).

The Muzaffarabad area was selected as a study site of the ReBuilDD (Remote sensing for Built environment Disaster and Development) (Brown et al. 2012) project because it was a major earthquake with severe damage The post disaster image was the first image we could find that was 100% cloud free. We chose the 100% cloud-free image in order to be able to visualize a large extent for proof of concept. Partially cloud covered images are available hours after a disaster and are recommended for disaster situations. There are also several satellite sensors that have compatible data that can be used together. De Alwis Pitts and So 2017 has shown the possibility of using multiple sensors (Geoeye-1, WorldView 2 etc.) for a similar change detection method for reads and open spaces.

The timing, the extent of the disaster and the fact that very little ground based data existed, made it a well suited as a case study of remotely sensed data. Though the pre disaster and post disaster image were taken 14 months apart, we didn’t see any new buildings built during that period. This is common in remote places. In the post disaster image that was taken 2 weeks after disaster it was evident that the damage to the building were still visible and the recovery process had not started.

Table1Imagery and Data Acquisition dates for Muzzaffarabad, Pakistan

Imagery	Acquisition Date
Pre-disaster(QuickBird)*	13th August 2004 – 14 months before earthquake
Post disaster 1(QuickBird) *	22nd October 2005 – 2 weeks after earthquake
Post disaster 2 (QuickBird) *	13th June 2006 – 8 months after earthquake

*QuickBird-2 imagery contained five bands namely Blue(450 - 520 nm), Green (520 - 600 nm), Red(630 - 690 nm), NIR(760 - 900 nm), and PAN (760 - 850 nm). The spectral bands have a resolution of 2.44 mand the PAN band has a pixel resolution of 0.61mnominal at nadir.

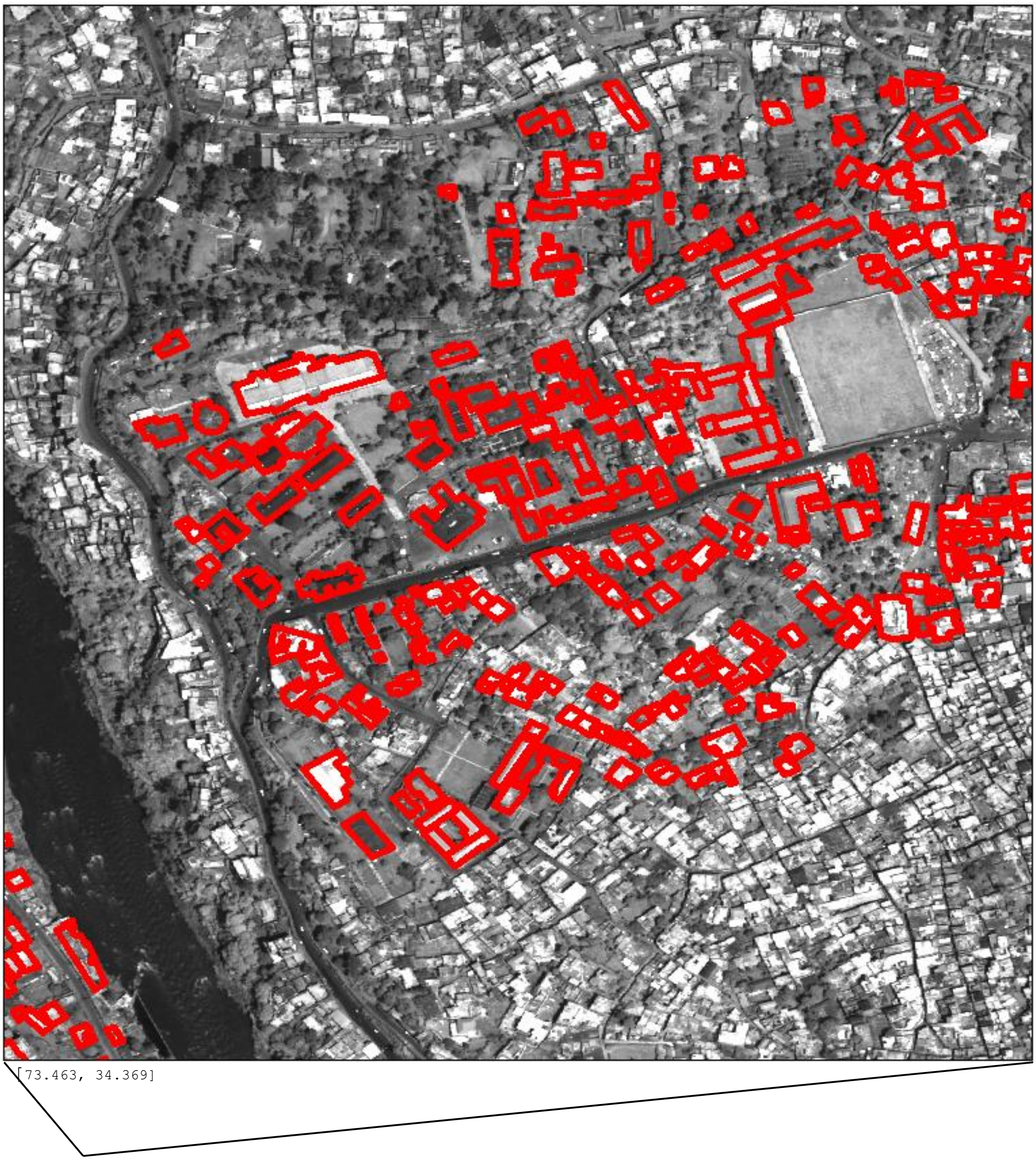

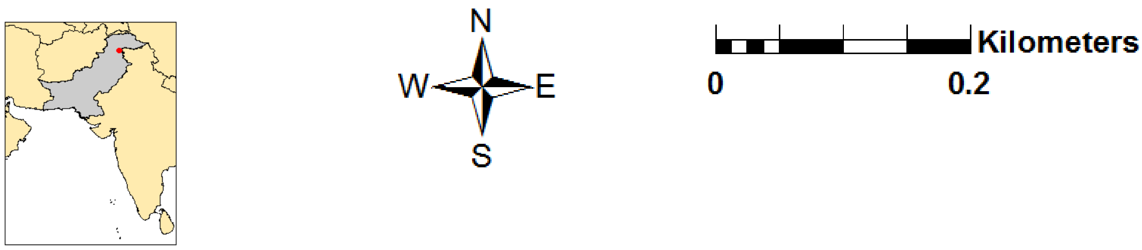

Figure 1 Study site, Muzzaffarabad, Pakistan . Shown in read are the screen digitised buildings.

2.2. Data Acquisition and Data Preparation

The process of initial data preparation for the proposed change detection method is shown in Figure 2. The following paragraphs explain the data preparation in detail.

Open Street Map data: The data pertaining to the road layer was downloaded directly from the Open Street Map (OSM) archive (GEOFABRIK (Download.geofabrik.de)). In the case of Muzzaffarabad, the street layers for the primary and secondary roads were manually digitised from the QuickBird VHR images using QGIS since the OSM data were incomplete.

Satellite Images: For the case study of Muzzaffarabad, three satellite images were acquired from 2004 to 2006 (Table1).

Geo-rectifying the pre-disaster image: All the satellite data were co-registered to the road layers obtained from OSM to ensure the best alignment (accuracy<1.47m). The pre-disaster IR R,G bands were first PAN-sharpened (using QGISOTB (OrfeoToolBox) Processing toolbox)and then co-registered to the road layer.

Geo-rectifying the post-disaster image: The PAN-sharpened post-disaster image was geo-rectified using buildings, roads, and junctions identified in both the pre and post images and used as ground control points.

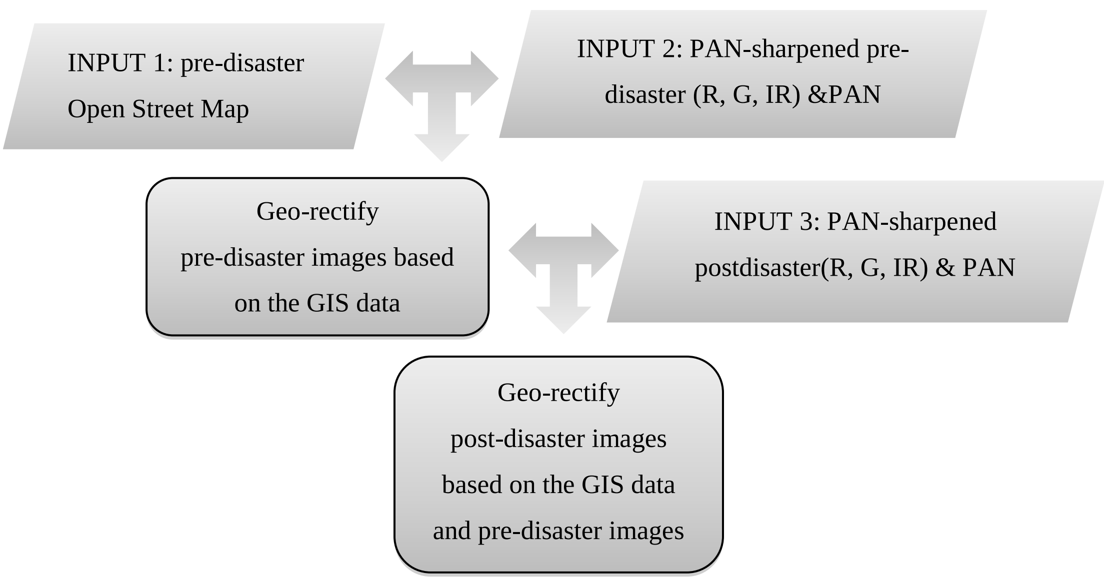

Figure 2 Data preparation workflow: Pre-disaster images are PAN-sharpened and geo-rectified to the Open Street Map and then the PAN-sharpened post-disaster images are geo-rectified to the pre-disaster images.

Screen Digitizing the Building

The buildings were digitized off the screen using QGIS from the pre disaster images. Only the area with damaged buildings and some of the surrounding buildings were digitized for this study. This is the only time consuming step in the analysis, having a pre disaster building GIS data for areas that are disaster prone would enable the analysis to proceed faster in case of a disaster.

Building the doughnut ring buffers around the buildings

In order to detect change in the edges of the buildings to determine structural changes that are indicative of damage buffers of a positive 1m and negative 1m were created around each building in the building layer. Then the negative buffers are deleted (erased) from the positive buffer to create a doughnut ring buffer around all the buildings.

Clipping the Building and the doughnut ring buffers

The geo-referenced, geo-rectified pre-post complete time series of images, are clipped by the building polygon and doughnut ring buffer layers. These layers are then used in the flowchart shown in Figure 3.

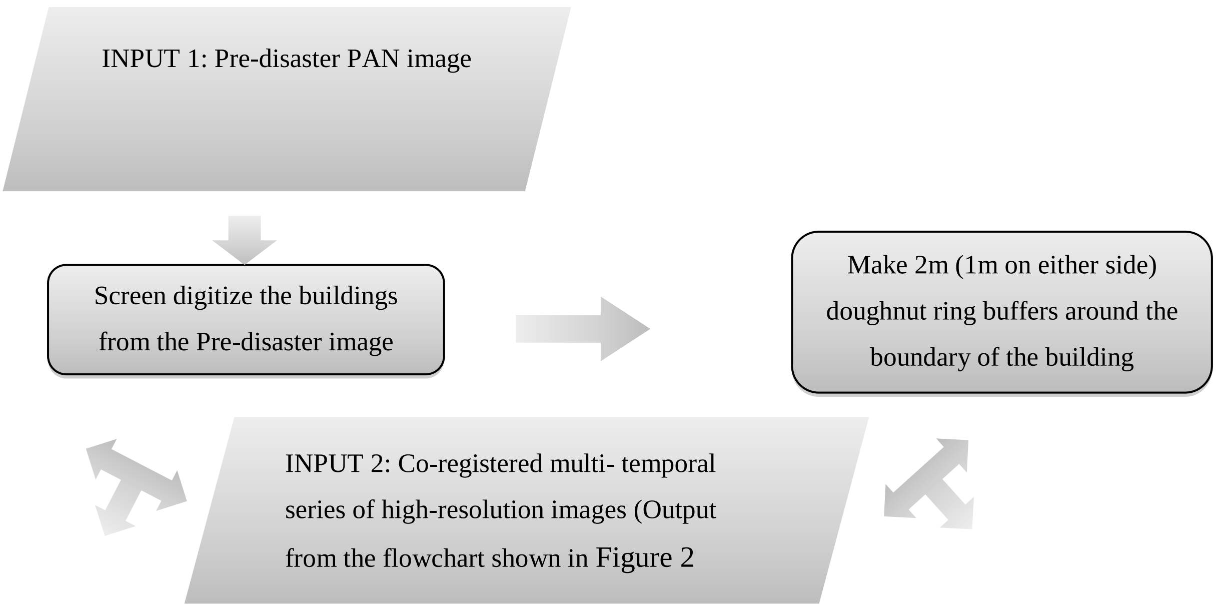

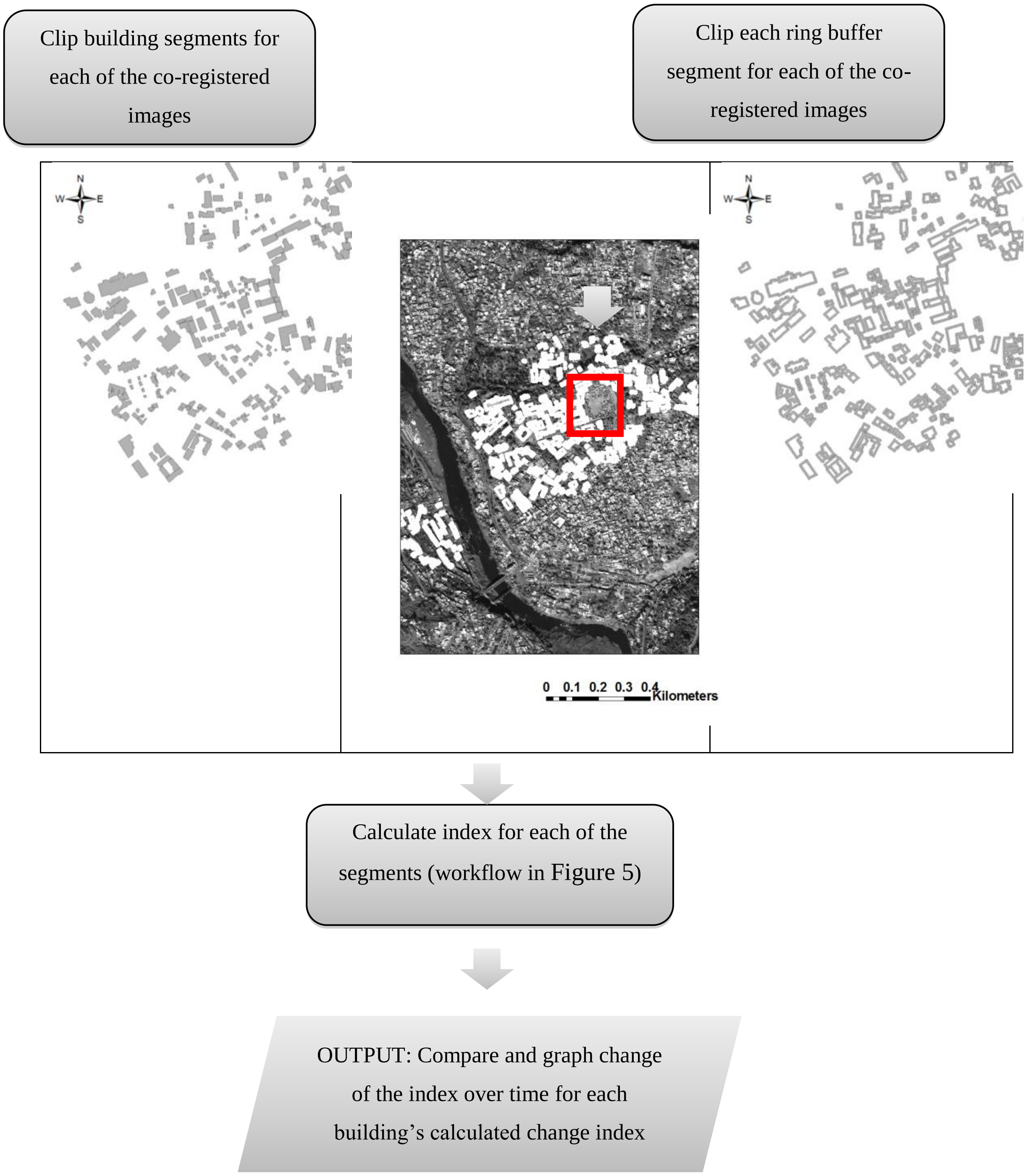

Figure 3 The workflow showing how the buildings (screen digitised GIS layers) and doughnut ring buffers of the building are used to clip the pre- and post-images. Then the clipped images are used to calculate the Enhanced Change Detection Index as per Figure 5

2.2.1. Pre-Post Normalized Difference of the Satellite data

As per workflow in Figure 5 the pre-post normalized difference between the PAN-sharpened, geo-referenced bands (R, G, IR) and PAN bands is calculated using Equation 1 for each building unit/segment. The pre-post normalized difference removes changes in reflectance due to acquisition times within the day. The normalized ratio in the denominator of Equation 1 helps to compensate for differences both in illumination within an image, and differences between images due to time of day or season when the images were acquired (Du et al., 2002). Taking the square root is intended to correct values approximate a Poisson distribution and introduce a normal distribution, producing a linear measurement scale (de Alwis Pitts and So 2007). Adding a constant of 0.5 to all pre-post normalized values does not always eliminate all negative values, but it leaves fewer of them.

$$\frac{\left(\frac{\boldsymbol{POST-PRE}}{\boldsymbol{POST+PRE}}+\mathbf{0.5}\right)}{\left|\left(\frac{\boldsymbol{POST-PRE}}{\boldsymbol{POST+PRE}}+\mathbf{0.5}\right)\right|}\cdot\sqrt{\left|\left(\frac{\boldsymbol{POST-PRE}}{\boldsymbol{POST+PRE}}+\mathbf{0.5}\right)\right|}$$ Equation 1

2.2.2. Enhanced Change Detection Index for Building Unit/Segment

As shown in Figure 4 each normalized difference of PAN and PAN-sharpened (IR, R, G) bands for each building segment was subjected to Vigra edge detection in QGIS (QGIS Development Team, 2015) and texture using GDAL’s (QGIS) roughness parameter. Edge filters of the pre-post normalized images were used to capture object specific changes in edges. Method derived for the roads and open spaces by de Alwis Pitts and So 2017 failed to be significantly correlated to the normalized gradient, texture and edges within the building as an object. The edges derived within the object as per de Alwis Pitts and So 2017 for roads failed for buildings because the edge patterns on some of the building roofs matched the rubble of the damaged buildings. Therefore, for buildings we modified the method used by de Alwis Pitts and So 2017 by making a doughnut shaped ring around the buildings to put more emphasis on capturing the change in the edges of the building which is indicative of structural damage. Changes in edges correlated well with the condition of the building and dominated the if the buildings were still standing.

Next the gradient is calculated for each object in pre- and post-images PAN sharpened bands (R, G, IR) and PAN bands and then normalized (for each band) using Equation 1. The change of edges, texture and gradient parameters are calculated within each of the objects as per the flowchart in Figure 6(building). This creates 12 change-related parameters (4 pertaining to edges, 4 to texture, and 4 to the gradient) for each object in regard to building segments.

a)	b)
	
	0 20 Meters
c)	d)
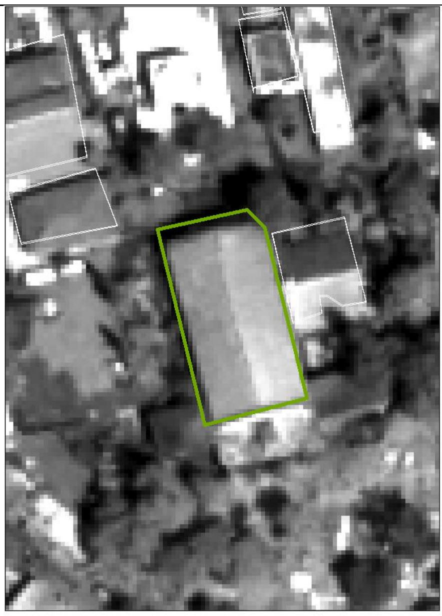	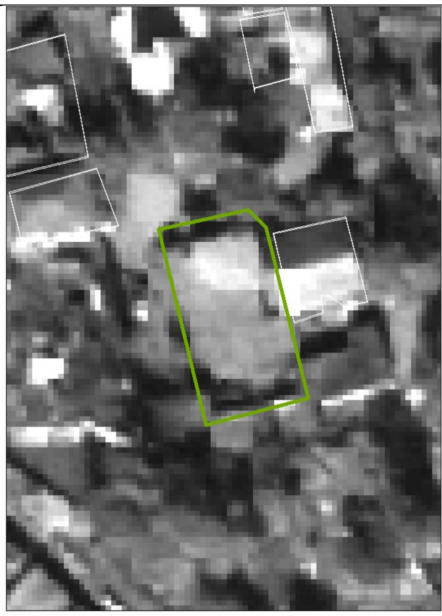

e)

f)

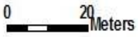

Figure 4 shows the zoomed in version of buildings in the pre (a, c, e)- and post-images (b, d, f). By looking at a) and b) images, a visual index of 2 was assigned because the aerial views of the buildings have not changed much between the two images. Images c) (pre) and d)(post) show a considerable change, hence a value of 5 is used as the visual index. As for the building shown in e) (pre) and f)(post) a visual index of 8 was assigned because more change is visible than the c) and d) images display.39 buildings were visually analysed and an appropriate visual index determined.

2.2.3. Visual Index (Training Data) for Building Unit/Segments

A visual index (VI) is developed by the user by comparing the pre and post images visually in a way that is analogous to a linear visual scale for change. The visual index is developed for 1/10th the buildings by looking at the zoomed in image of the same building in the pre and post disaster image back and forth. This can be done in a GIS software overlaying the pre and post images one on top of the building layer other. By looking at the zoomed in view of the building a value ranging from 1-10 is assigned to represent the change of the building. When a single user develops the VI it has been seen to be consistent (de Alwis Pitts and So. 2017) throughout the task. As shown in Figure 4, the building segments that had mild changes were assigned a small VI (close to 0, Figure 7 a) and b)) and the segments that showed large changes were assigned large VI values (close to 10, Figure 4c) and d)).

Then as seen in Figure 5, this visual index was used as a training set and regressed against the derived values of pre-post normalized gradient, edges, and roughness of each building segment.

INPUT I: Building segments of the co-registered pre-disaster image

INPUT 3: Building ring buffer segments of the co-registered pre-disaster image

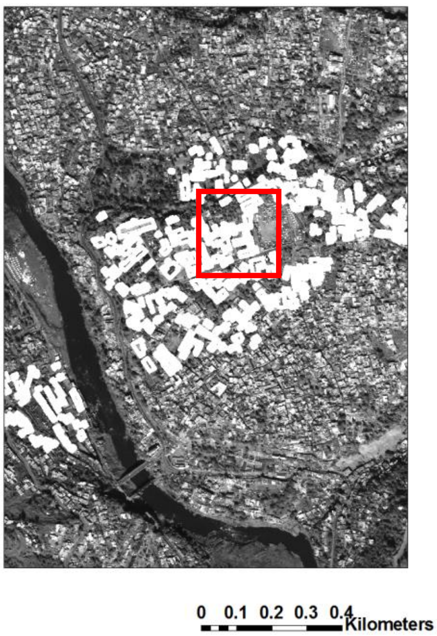

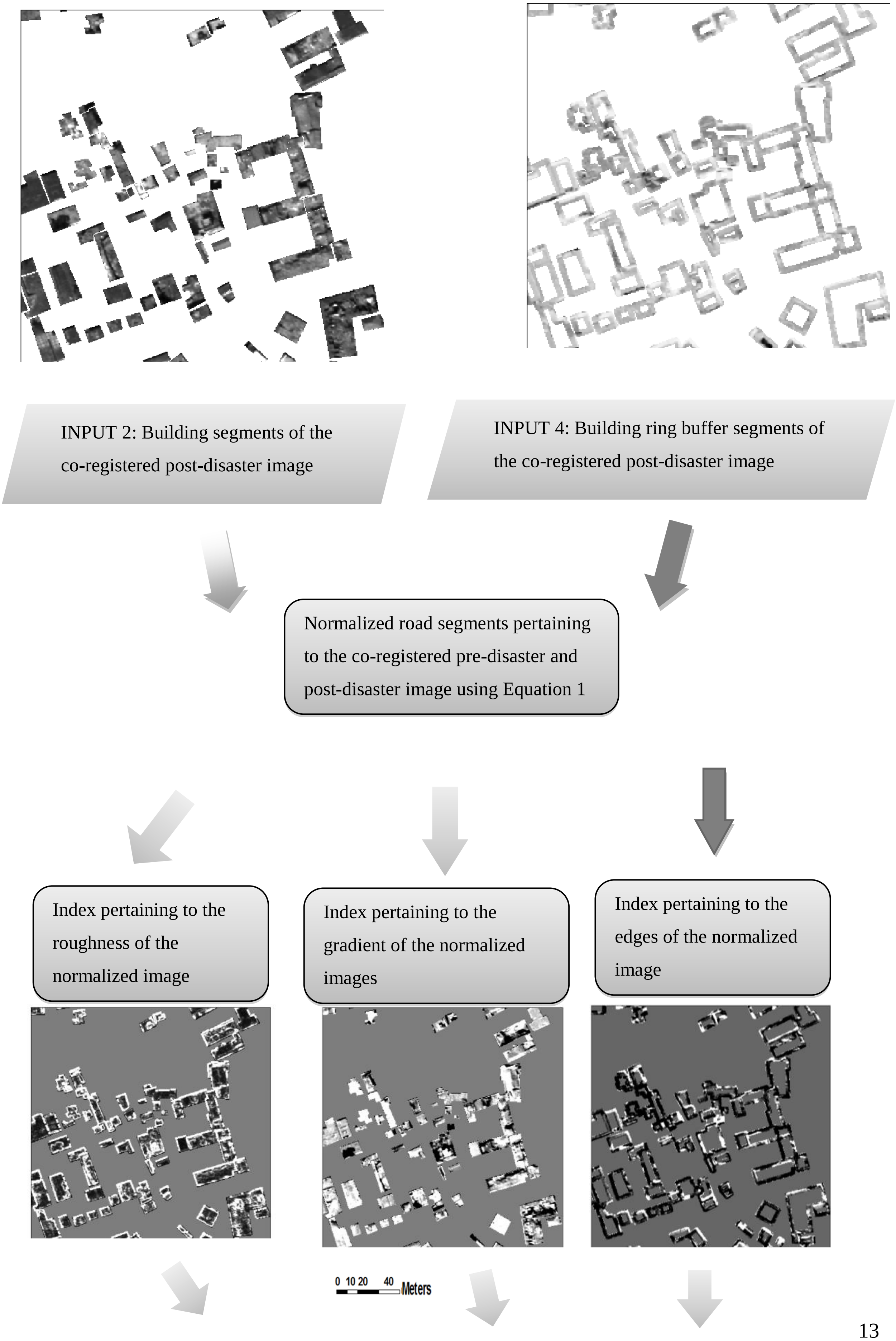
INPUT 2: Building segments of the co-registered post-disaster image
INPUT 4: Building ring buffer segments of the co-registered post-disaster image
Normalized road segments pertaining to the co-registered pre-disaster and post-disaster image using Equation 1
Index pertaining to the roughness of the normalized image
Index pertaining to the gradient of the normalized images
Index pertaining to the edges of the normalized image
0 10 20 40 Meters

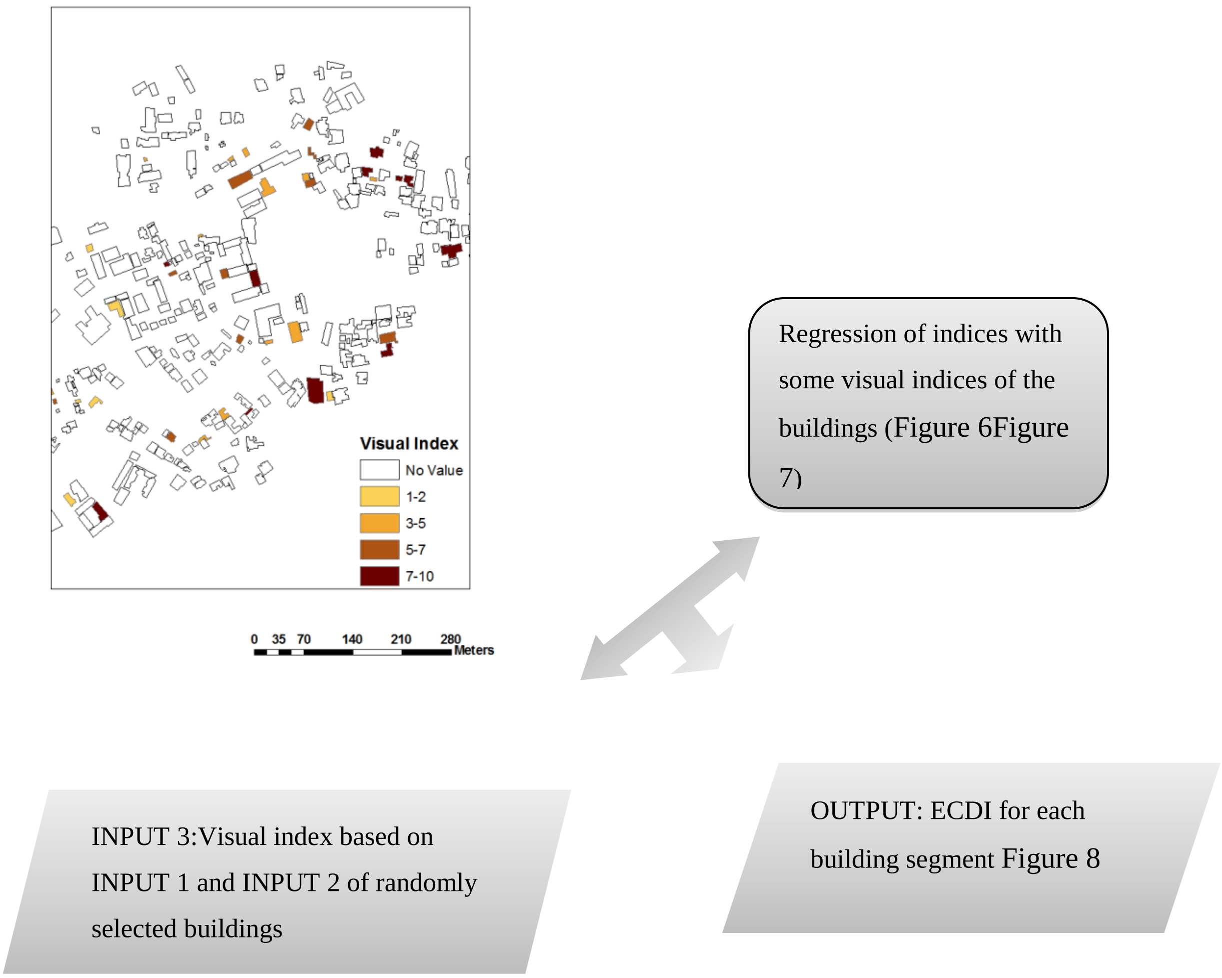

Figure 5 Workflow showing the enhanced change detection index(ECDI)for the buildings in Muzzaffarabad. The pre- and post-disaster images (outputs from the workflow shown in Figure 2) are normalized and a value pertaining to the roughness, gradient is calculated for each building segment and edges from its doughnut ring buffer. The change-related parameters (texture, gradient and edges) for each building segment is then regressed with the visual index to find the coefficients to create the ECDI.

2.2.4. Regression

We use regression analysis for estimating the relationship among the roughness, gradient and edge parameters to quantify change. The regression model predictors are the roughness, gradient and edges of the buildings and the independent variable is the change index (ECDI). We use a visual index (VI) for 10% of the buildings to train the algorithm. Then using the coefficients obtained from the training data a change index (ECDI) is obtained for the data. The derived coefficients are again used to create the change index for the 10 percent of the data used to train the data. The derived change index obtained for the data used for the training is analysed against the visual index to see they are roughly proportional.

The visual index derived by observing the visual changes in pre- and post-disaster images for 39 building units were regressed with the values obtained from change in texture, gradient, and edges.

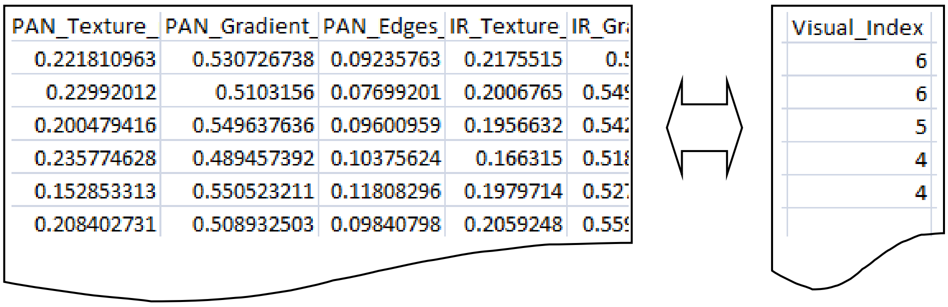

Figure 6 The calculated normalized texture, gradient and edge values derived for each building object for(R, G, IR) and PAN bands are regressed with the visual index obtained by observing the visual changes in pre- and post-disaster images for 1/10th of the building segments. The obtained regression coefficients are then used to calculate the ECDI (enhanced change detection index) for all the roads.

The R square value was 0.72 with low P values (varied from 0.0000443 to 0.014) for PAN and PAN-sharpened IR bands derived gradient, texture, and edge parameter. This low P value with a high R square combination indicates that changes in the predictors (gradient, texture, and edge) are related to changes in the response variable (visual index), thereby indicating that the model explains a great dealof the response variability. Red and green band derived parameters did not contribute significantly. The graph of the visual index *vs*. ECDI is shown in Figure 7.

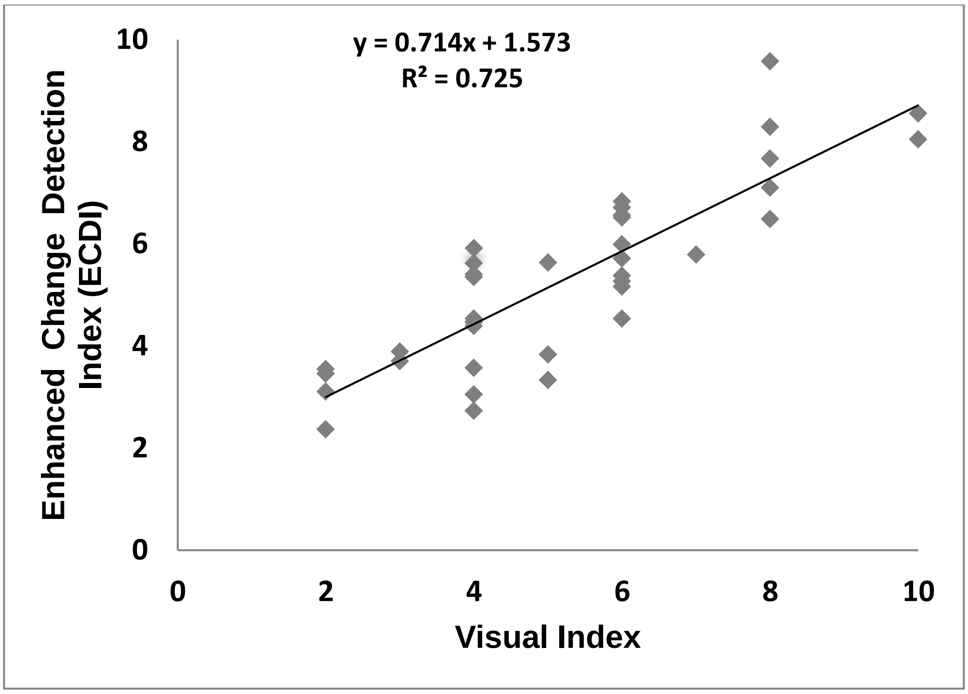

Figure 7: The visual index (using Figure 4*vs.* the calculated ECDI (enhanced change detection index) (Figure 6) for the selected building segments. The figure shows a good correlation between the visual index and the pre- and post-disaster normalized parameters (texture, edges, and gradient) for the building segments and the doughnut ring buffers to create ECDI.

3. Results

The pre/post normalized relative change (ECDI) for the building segments in Muzaffarabad is shown in Figure 8: The higher ECDI indicates a significant change, implying that the buildings have changed since the disaster when compared to the pre-disaster image. Knowing which buildings have changed relative to the other buildings can allow emergency responses to determine critical areas and mange response teams and resources. Here it is necessary to mention that the change is based on nadir view, and so is only indicative of change in roof and walls visible to a nadir view. This is not really a limit of the methodology because it is common to all passive remotely sensed data available soon after a disaster in data poor countries.

Obtaining information with regards to the operational status of critical facilities and lifelines networks is certainly a crucial requirement for end-users. Remote sensing technologies can offer means to gauge detailed information about such infrastructure, and most often the operational status of such facilities can only be directly verified with in-situ surveys

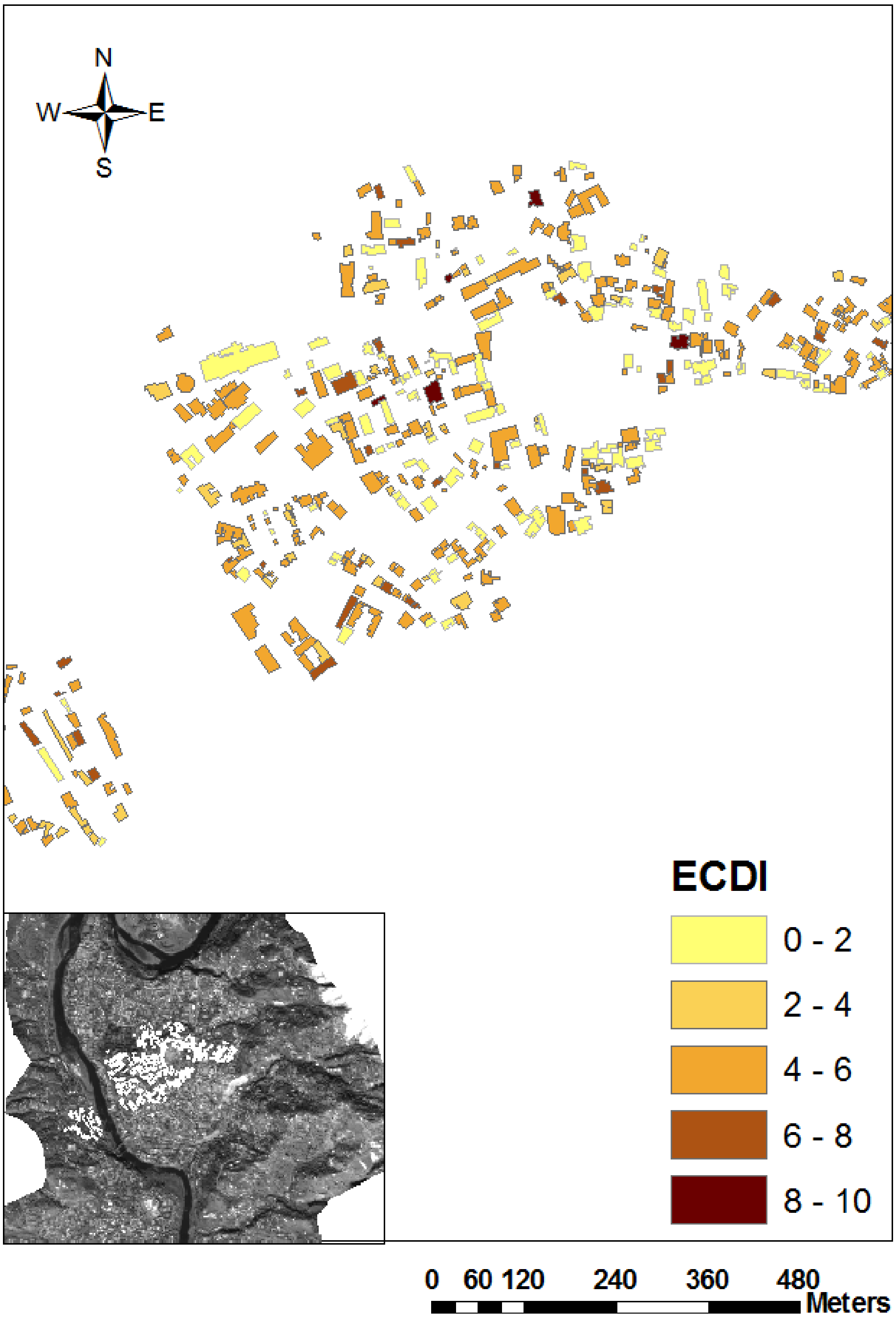

Figure 8: Enhanced change detection index (ECDI) for buildings obtained from pre-disaster and post-disaster. Higher indices (represented by darker colors) indicate greater changes after disaster.

As shown in **Error! Reference source not found.**, each image can be compared to the pre-disaster image as well as an image immediately following a post-disaster image to get a better picture of the recovery situation.

Case Study Scenarios

Error! Reference source not found. outlines scenarios that can be seen when ECDIs are observed over time. They are obtained by comparing post-disaster images to pre-disaster image.

ECDI of Pre disaster & Post T1[*]	ECDI of Pre disaster & Post T2[*]	ECDI of Post T1[*]& Post T2[*]	Scenario
>5	<5	>5	Building affected by post T1 date and recovered by Post T2 date
>5	>5	<5	Building affected by post T1 date and NOT recovered by Post T2 date
<5	<5	<5	Building not affected
<5	>5	>5	Buildingnot affected by post T1 data and not modified by Post T2 date

[*]Post T1 and Post T2 are dates after the disaster.

As seen in **Error! Reference source not found.**, by obtaining the ECDI for the two post-disaster images and then comparing them to the pre-disaster image, we were able to identify buildings that were rebuilt after disaster. With more post-disaster images, a progressive recovery can be observed.

4. Discussion and conclusions

The proposed method uses GIS objects and integrates existing knowledge into processing to optimize change detection. This change detection method uses the calculation of the texture, edges, and gradient of each object to better estimate the change between the pre- and post-disaster data. To determine what proportions of each of the above properties contribute to real change, a visual index is used to train the data. Like any user-derived parameter, the visual index can be very specific to the user. However, provided that the visual index is completed by a single user, it should contain relative differences representative of the changes within the image (de Alwis Pitts and So 2017). It is easy to visually see objects that underwent a large change and those that experienced no change, so more objects at extremes were used for the visual index. It is best to use more objects at the ends of the change spectrum because the computer is then better able to estimate objects that are at different gradients of change.

The normalization between the pre- and post-disaster data reduces the differences caused due to the acquisition times and atmospheric anomalies of the pre/post images. The VHR sensors used in this study collect data around the same time, so the shadow effect due to acquisition time will be minimal; the main issues are the incidence angle and changes in solar zenith, because these will impact the imagery more directly than the difference between acquisition times. The considered relative change by normalizing between the pre- and post-images would give more weight to the changes and less to the increase and decrease in shadows.

Once the change is quantified based on training data, the pre/post normalized method outlined in this paper can be used automatically to detect change and to observe recovery over time. Comparing the most recent image and consecutive past images can give a complete history of changes pertaining to the buildings. As demonstrated for roads by de Alwis Pitts and So 2017, another benefit is that this method can be potentially applied over large areas to get the big picture and to determine changes over time.

After obtaining the imagery, provided there is a GIS layer of the buildings, it takes 1-2 hours to create training data, then it takes 2-3 more hours to co-register the images and run the algorithm. Overall the processing in this method, from training to the final deliverables, takes 3-5 hours. The most time-consuming step is obtaining the pre-disaster building layer through screen digitising when pre-disaster GIS data are not available. We highly recommend that the GIS data be collected, updated and be ready to use in disaster prone areas in order to benefit from this method. Provided the GIS data and the images are available the proposed method can be executed in a semi-automated way within hours to identify focus areas.

If further information is known about the buildings, then the information could be used to categorize the building into classes based on the building construction material (Carrasco et al. 2017). Buildings with similar construction material would have similar texture, reflectance gradient, and edges, and so would disintegrate similarly under similar stresses. Categorising buildings based on the roof types and building material would increase the accuracy of the method. The grouping should also consider the age of the buildings, which is indicative of destruction thresholds. Subcategorizing buildings would increase the ability to detect changes more accurately because of the similarity in texture, reflectance gradient, and edges. If further ground information is not available, assuming that the colour of the roof is indicative of the building material could be an initial step in categorising the building. It should be noted that the nadir view of the building observed using passive VHR sensors only lets us see the condition of the roof, but the roof seen in a nadir view is not always indicative of the damage occurred to the building. However, given that VHR images could be obtained immediately after a disaster in data poor countries, VHR images are a good resource to be used by emergency responders for mapping out the damage.

Roofs obscured by tree cover showed false change situations when only the tree got destroyed after the disaster. Further improvements could be achieved by using the NDVI (Normalised Difference Vegetation Index) since this would allow to subtract the vegetation cover over building segments. In our case study there were very few trees over the roofs, so tree cover was not a major issue. We were able to avoid the trees by digitising around them.

The coefficients pertaining to the texture, edges, and gradient obtained from the visual index are transferable to other buildings with similar construction material and thus similar reflective properties. This transferability works better for buildings that are categorized into finer classes and are analysed separately. The ECDI can be used during the recovery to observe change and recovery after disaster. This change is a good indicator of recovery over time after disaster. The houses can be separated to zones for zonal statistics to observe the change from the epicentre of disaster or differences of urban and sub-urban recovery differences over time. The method used in this paper uses QGIS, free software which is thus appropriate for the use in developing countries with limited resources.

This research was partly supported by the European Commission under FP7 (Seventh Framework Programme): “SENSUM: Framework to Intergrade Space-based and in-situ sENSing for dynamic vUlnerability and recovery Monitoring” (312972). We gratefully acknowledge the contributionfrom the anonymous referees.

References

Akcay, H.G. and S. Aksoy. 2008. "Automatic Detection Of Geospatial Objects Using Multiple Hierarchical Segmentations". *IEEE Transactions On Geoscience And Remote Sensing* 46 (7): 2097-2111. doi:10.1109/tgrs.2008.916644.

Al-Khudhairy, D.H.A., I. Caravaggi, and S. Giada. 2005. "Structural Damage Assessments FromIkonos Data Using Change Detection, Object-Oriented Segmentation, And Classification Techniques". *Photogrammetric Engineering & Remote Sensing* 71 (7): 825-837. doi:10.14358/pers.71.7.825.

Bird, Juliet F. and Julian J. Bommer. 2004. "Earthquake Losses Due To Ground Failure". *Engineering Geology* 75 (2): 147-179. doi:10.1016/j.enggeo.2004.05.006.

Blaschke, T. 2010. "Object Based Image Analysis For Remote Sensing". *ISPRS Journal Of Photogrammetry And Remote Sensing* 65 (1): 2-16. doi:10.1016/j.isprsjprs.2009.06.004.

Brown, D., Bevington, J., Platt, S., Saito, K., Adams, B. J., Chenvidyakarn, T., Spence, R. J., Chuenpagdee, R., Khan, A., So, E., (2012) “Monitoring and Evaluating Post-Disaster Recovery Using High-Resolution Satellite Imagery – Towards Standardised Indicators for Post-Disaster Recovery”, ReBuilDD Workshop, Cambridge, UK.

Carrasco, E. V. M., Magalhaes, M. D. C., Santos, W. J. D., Alves, R. C., Mantilla, J. N. R., (2017) Characterization of mortars with iron ore tailings using destructive and nondestructive tests. *Construction and Building Materials 131 (2017) 31-38.*

Cheng, Gong and Junwei Han. 2016. "A Survey On Object Detection In Optical Remote Sensing Images". *ISPRS Journal Of Photogrammetry And Remote Sensing* 117: 11-28. doi:10.1016/j.isprsjprs.2016.03.014.

de Alwis Pitts, Dilkushi A. and Emily So. 2017. "Enhanced Change Detection Index For Disaster Response, Recovery Assessment And Monitoring Of Accessibility And Open Spaces (Camp Sites)". *International Journal Of Applied Earth Observation And Geoinformation*57: 49-60. doi:10.1016/j.jag.2016.12.004.

Du, Yong, Philippe M Teillet, and Josef Cihlar. 2002. "Radiometric Normalization Of Multitemporal High-Resolution Satellite Images With Quality Control For Land Cover Change Detection". Remote Sensing Of Environment 82 (1): 123-134. doi:10.1016/s0034-4257(02)00029-9.

Earthquake.usgs.gov,. 2005. 'PAKISTAN'.http://earthquake.usgs.gov/earthquakes/eqinthenews/2005/usdyae/#details.

Edrissi, Ali, Hossain Poorzahedy, HabibollahNassiri, and Mehdi Nourinejad. 2013. "A Multi-Agent Optimization Formulation Of Earthquake Disaster Prevention And Management".

European Journal Of Operational Research 229 (1): 261-275. doi:10.1016/j.ejor.2013.03.008.

Gerke, M. and Kerle, N. 2011b. "Graph matching in 3D space for structural seismic damage assessment". *IEEE International Conference on Computer Vision Workshops* (ICCV Workshops), Barcelona, 204–211.

Guo, Zhou, Shihong Du, Mei Li, and Wenzhi Zhao. 2015. "Exploring GIS Knowledge To Improve Building Extraction And Change Detection From VHR Imagery In Urban Areas". International Journal Of Image And Data Fusion 7 (1): 42-62. doi:10.1080/19479832.2015.1051138.

Haala, Norbert and Claus Brenner. 1999. "Extraction Of Buildings And Trees In Urban Environments". *ISPRS Journal Of Photogrammetry And Remote Sensing* 54 (2-3): 130-137. doi:10.1016/s0924-2716(99)00010-6.

Hofmann, A.D., Maas, H.-G., Streilein, A., 2002.“Knowledge-based building detectionbased on laser scanner data and topographic map information.*”Int. Arch.Photogramm. Remote Sens. Spat. Inform. Sci.* 34, 169–174.

Huertas, A and R Nevatia. 1988. "Detecting Buildings In Aerial Images". *Computer Vision, Graphics, And Image Processing* 41 (2): 131-152. doi:10.1016/0734-189x(88)90016-3.

Irvin, R.B. and D.M. McKeown. 1989. "Methods For Exploiting The Relationship Between Buildings And Their Shadows In Aerial Imagery". *IEEE Transactions On Systems, Man, And Cybernetics* 19 (6): 1564-1575. doi:10.1109/21.44071.

Kerle, Norman. 2010. "Satellite-Based Damage Mapping Following The 2006 Indonesia Earthquake—How Accurate Was It?".*International Journal Of Applied Earth Observation And Geoinformation* 12 (6): 466-476. doi:10.1016/j.jag.2010.07.004.

Kumar, S., Hebert, M., 2003.“Discriminative random fields: a discriminativeframework for contextual interaction in classification.” In: Proc. *IEEE Int. Conf. Comput. Vis.,* pp. 1150–1157.

Lafferty, J., McCallum, A., Pereira, F.C., 2001. “Conditional random fields: probabilisticmodels for segmenting and labeling sequence data.”*In: Proc. Int. Conf. Mach.Learn.,* pp. 282–289.

Lefèvre, S., Weber, J., Sheeren, D., 2007. “Automatic building extraction in VHR images using advanced morphological operators”. In: Proc. *Urban Remote Sens.* Joint Event, 1-5.

LI, XIAODONG, WUNIAN YANG, TIANQI AO, HONGXIA LI, and WENQING CHEN. 2011. "AN IMPROVED APPROACH OF INFORMATION EXTRACTION FOR EARTHQUAKE-DAMAGED BUILDINGS USING HIGH-RESOLUTION IMAGERY". *Journal Of Earthquake And Tsunami* 05 (04): 389-399. doi:10.1142/s1793431111001157.

Lin, Chungan and RamakantNevatia. 1998. "Building Detection And Description From A Single Intensity Image". *Computer Vision And Image Understanding* 72 (2): 101-121. doi:10.1006/cviu.1998.0724.

Lin, Chungan and RamakantNevatia. 1998. "Building Detection And Description From A Single Intensity Image". *Computer Vision And Image Understanding* 72 (2): 101-121. doi:10.1006/cviu.1998.0724.

Liow, Yuh-Tay and Theo Pavilidis. 1989. "Use Of Shadows For Extracting Buildings In Aerial Images". *Computer Vision, Graphics, And Image Processing* 48 (2): 280. doi:10.1016/s0734-189x(89)80047-7.

Lhomme , S. Dong-Chen He , C. Weber & D. Morin.2009 ”A new approach to building identification from very-high-spatial-resolution images”. *International Journal of Remote Sensing*.30, 5

McGlone, J.C., Shufelt, J., 1994. “Projective and object space geometry for monocularbuilding extraction.” In: Proc. *IEEE Int. Conf. Comput. Vis. Pattern Recognit*., pp.54–61.

Michaelsen, Eckart, Uwe Soergel, and Ulrich Thoennessen. 2006. "Perceptual Grouping For Automatic Detection Of Man-Made Structures In High-Resolution SAR Data". *Pattern Recognition Letters* 27 (4): 218-225. doi:10.1016/j.patrec.2005.08.002.

Ok, Ali Ozgun. 2013. "Automated Detection Of Buildings From Single VHR Multispectral Images Using Shadow Information And Graph Cuts". *ISPRS Journal Of Photogrammetry And Remote Sensing* 86: 21-40. doi:10.1016/j.isprsjprs.2013.09.004.

Ok, Ali Ozgun, CaglarSenaras, and BarisYuksel. 2013. "Automated Detection Of Arbitrarily Shaped Buildings In Complex Environments From Monocular VHR Optical Satellite Imagery". *IEEE Transactions On Geoscience And Remote Sensing* 51 (3): 1701-1717. doi:10.1109/tgrs.2012.2207123.

Pagot, E., M. Pesaresi, D. Buda, and D. Ehrlich. 2008. "Development Of An Object-Oriented Classification Model Using Very High Resolution Satellite Imagery For Monitoring Diamond Mining Activity". *International Journal Of Remote Sensing* 29 (2): 499-512. doi:10.1080/01431160601047771.

Peng, J. and Y. C. Liu. 2005. "Model And Context-Driven Building Extraction In Dense Urban Aerial Images". *International Journal Of Remote Sensing* 26 (7): 1289-1307. doi:10.1080/01431160512331326675.

Peng, J., Zhang, D., Liu, Y., 2005a." An improved snake model for building detectionfrom urban aerial images."*Pattern Recognit.Lett*. 26, 587–595.

QGIS Development Team, 2015.QGIS Geographic Information System Developers Manual. Open Source Geospatial Foundation Project. Electronic document: http://www.qgis.org/wiki/Developers_Manual

Senaras, Caglar, Mete Ozay, and Fatos T. YarmanVural. 2013. "Building Detection With Decision Fusion". *IEEE Journal Of Selected Topics In Applied Earth Observations And Remote Sensing* 6 (3): 1295-1304. doi:10.1109/jstars.2013.2249498.

Shufelt, J.A., 1996. “Exploiting photogrammetric methods for building extraction inaerial images.”*Int. Arch. Photogramm. Remote Sens.* 31, B6.

Sirmacek, B., and C. Unsalan. 2009. "Urban-Area And Building Detection Using SIFT Keypoints And Graph Theory". *IEEE Transactions On Geoscience And Remote Sensing* 47 (4): 1156-1167. doi:10.1109/tgrs.2008.2008440.

Stankov, Katia and Dong-Chen He. 2013. "Building Detection In Very High Spatial Resolution Multispectral Images Using The Hit-Or-Miss Transform". *IEEE Geoscience And Remote Sensing Letters* 10 (1): 86-90. doi:10.1109/lgrs.2012.2193552.

Stankov, Katia and Dong-Chen He. 2014. "Detection Of Buildings In Multispectral Very High Spatial Resolution Images Using The Percentage Occupancy Hit-Or-Miss Transform". *IEEE Journal Of Selected Topics In Applied Earth Observations And Remote Sensing* 7 (10): 4069-4080. doi:10.1109/jstars.2014.2308301.

Stilla, U., Geibel, R., Jurkiewicz, K., 1997. “Building reconstruction using different views and context knowledge”.*Int. Arch. Photogramm. Remote Sens.* 32, 129–136.

Vetrivel, Anand, Markus Gerke, Norman Kerle, and George Vosselman. 2015. "Identification Of Damage In Buildings Based On Gaps In 3D Point Clouds From Very High Resolution Oblique Airborne Images". *ISPRS Journal Of Photogrammetry And Remote Sensing* 105: 61-78. doi:10.1016/j.isprsjprs.2015.03.016.

Vu, T. T. and Y. Ban. 2010. "Context-Based Mapping Of Damaged Buildings From High-Resolution Optical Satellite Images". *International Journal Of Remote Sensing* 31 (13): 3411-3425. doi:10.1080/01431161003727697.

Walter, Volker. 2004. "Object-Based Classification Of Remote Sensing Data For Change Detection". *ISPRS Journal Of Photogrammetry And Remote Sensing* 58 (3-4): 225-238. doi:10.1016/j.isprsjprs.2003.09.007.

Weidner, Uwe and W. Förstner. 1995. "Towards Automatic Building Extraction From High-Resolution Digital Elevation Models". *ISPRS Journal Of Photogrammetry And Remote Sensing* 50 (4): 38-49. doi:10.1016/0924-2716(95)98236-s.

XiaolongDai, and S. Khorram. 1998. "The Effects Of Image Misregistration On The Accuracy Of Remotely Sensed Change Detection". *IEEE Transactions On Geoscience And Remote Sensing* 36 (5): 1566-1577. doi:10.1109/36.718860.